

Ultrafast Photodissociation Dynamics of Ni(CO)₄W. Fuss,^{*,†} W. E. Schmid,[†] and S. A. Trushin^{†,‡}*Max-Planck-Institut für Quantenoptik, D-85741 Garching, Germany, and B.I. Stepanov Institute of Physics, Belarus Academy of Sciences, 220602 Minsk, Belarus**Received: June 27, 2000; In Final Form: November 1, 2000*

By time-resolved nonresonant (800 nm) multiphoton ionization we found six consecutive exponential processes after excitation of Ni(CO)₄ at 267 nm in the gas phase. Up to four steps (time constants 22 to 70 fs) probably correspond to relaxation and internal conversion between metal-to-ligand charge-transfer states in the intact molecule. Only the next step (600 fs) represents elimination of a CO group. This is an order of magnitude slower than in most other metal carbonyls investigated so far. The dissociation product is Ni(CO)₃ in its S₁ state. It does not relax to the ground state but luminesces (probably after intersystem crossing). This implies the absence of an easily accessible S₁/S₀ conical intersection. Such an intersection is induced by the Jahn–Teller effect in other carbonyls (which therefore do not luminesce), but not in Ni(CO)₃. To explain a pump–wavelength-dependent time constant (42, 55, and 113 ps at 260, 267, and 276 nm, respectively), we assume that part of Ni(CO)₃ dissociates to electronically excited Ni(CO)₂, which has probably slightly higher energy. Although the case of tetracarbonyl nickel superficially looks very different from that of other metal carbonyls, there are many similarities of the detailed pathway.

Introduction

On excitation in the near ultraviolet (UV), simple metal carbonyls M(CO)_n photochemically eliminate a single CO.^{1,2} Depending on the excitation wavelength and the associated excess energy, in the hot S₀ state further carbonyl groups may be split off from M(CO)_{n–1} in the gas phase, whereas in the condensed phase this step is suppressed by cooling. As shown by ultrafast spectroscopy [Cr(CO)₆,³ M(CO)₆,⁴ Fe(CO)₅,⁵ survey⁶], several phases can already be distinguished in the photochemical part: The intact molecules relax from the initially excited metal-to-ligand charge-transfer (MLCT) state via conical intersections to one of the lowest such states, from where they find their way typically via an avoided crossing to a repulsive surface belonging to a d → d (ligand-field, LF) excited state; the dissociation product M(CO)_{n–1} is initially in its first excited singlet state, but relaxes from there to S₀ through a Jahn–Teller (JT)-induced conical intersection in a time below 100 fs. This mechanism is in agreement with modern quantum chemical calculations,^{7–10} although there are slight deviations in detail and although theory still has difficulties with the many close-lying excited states. Ultrafast work on other metal carbonyls is discussed in our previous papers.^{3–5} A review of relevant work is also given in ref 11.

A conspicuous difference from other carbonyls is the luminescence observed on UV irradiation of Ni(CO)₄.^{12–14} It was assigned to the dissociation product Ni(CO)₃.^{12,13,15} We explained the absence of an analogous luminescence in other carbonyls by the ultrafast S₁ → S₀ relaxation through the JT-induced conical intersection mentioned above.^{3–6} In this work we show that the JT effect indeed does not provide an easily accessible analogous intersection in Ni(CO)₃. Daniel et al.¹⁶ pointed in this context to another difference in the unsaturated

carbonyls: Fe(CO)₄ has a triplet ground state directly correlating with a triplet excited Fe(CO)₅ state. This is in contrast to Ni(CO)₃, Cr(CO)₅, and others that were predicted to be formed in the S₁ state. But the postulated triplet participation is not a satisfactory explanation for why there is no luminescence in the iron system since it cannot apply to the unsaturated carbonyls of, for example, the group-6 metals, which have singlet ground states, but do not luminesce either.

Hepburn and co-workers investigated photofragment spectroscopy of Ni(CO)₄.¹⁷ The measured distributions over translational, rotational, and vibrational energies of the product CO could be characterized by temperatures. To model these distributions, the authors had to assume that the unsaturated nickel carbonyl is formed in an electronically excited state with high quantum yield that depended on the excitation wavelength.

Another difference between Ni(CO)₄ and other carbonyls is that the former has no LF transitions because Ni has a full d shell. This could be of importance for photochemistry because the LF surfaces, which steeply decline from initially high energies, control the final phase of dissociation in other carbonyls.^{3,4,7,8} On the other hand, a SAC-CI calculation for Ni(CO)₄¹⁵ predicted that states involving excitation to a higher shell such as d → 4s are at similar energies and can play a similar role for dissociation as the LF states for other carbonyls. This work also investigated potential energy curves along the Ni–CO dissociation coordinate, calculated the first excited state of Ni(CO)₃, and pointed out the role of the JT effect in this unsaturated carbonyl. A CAS-PT2 calculation for Ni(CO)₄ predicted 14 singlet MLCT transitions (4 of them symmetry allowed, species T₂ in T_d) with energies below about 6.2 eV (200 nm)⁹ and on this basis assigned the UV spectrum (gas phase,¹⁸ solution;¹⁹ see also Figure 1 below). Our pump laser (267 nm, 4.65 eV) excites the first allowed transition (to 1T₂). Below this energy three more singlet states are predicted down to 3.5 eV.⁹ In the SAC-CI calculation¹⁵ there are only two states below 1T₂ with energies down to 4.5 eV. This is less well in agreement with the spectrum that extends to about 3.2 eV (390

* Author for correspondence. Fax: +49-89-32905-200; e-mail: w.fuss@mpq.mpg.de.

[†] Max-Planck-Institut für Quantenoptik.

[‡] B.I. Stepanov Institute of Physics.

nm). Also, the previous CAS-PT2 calculation without correlation to core electrons²⁰ and a time-dependent density functional theory (DFT) calculation²¹ show more deviations from the spectrum.

As in our previous work on metal carbonyls,^{3–6} we investigated Ni(CO)₄ after pumping at 267 nm with time resolution²² in the femtosecond range by transient nonresonant (800 nm) photoionization with mass-selective determination of the ion yields as function of the pump–probe delay time. An advantage of this method (over transient absorption, for instance) is that it provides many time constants that correspond to lifetimes of, or traveling times through, consecutive locations (observation windows) on the potential energy surface(s). (Note that these surfaces extend from the reactant to the product.) Although the assignment of these locations is usually not trivial, it is possible to monitor the molecule’s pathway all along the potential energy surfaces down to the ground state of the product (e.g., in refs 3–5 and 23). A detailed discussion of the method including experimental details can be found in ref 23 and a comparison with transient absorption in refs 22 and 24.

Experimental Method

The experiments were carried out in the widely used pump–probe setup with a Ti:sapphire oscillator–amplifier system and a linear time-of-flight mass spectrometer described elsewhere,²³ briefly also in refs 3 and 5. Ni(CO)₄ was investigated in the gas phase at room temperature at a pressure of 10^{−7} mbar maintained by introducing it through a precision valve. It was excited by pulses at 267 nm (in some experiments at 260 and 276 nm) with an energy density around 0.1 mJ cm^{−2} (intensity 10⁹ W cm^{−2}), much below the saturation energy of about 35 mJ cm^{−2}. To probe the excited molecules, we used delayed 800-nm pulses with intensity around 3 × 10¹² W cm^{−2} in the focal plane and a full width at half-maximum of 110 fs. The pump pulse duration was 110 fs, too, as determined from the width of the Cr(CO)₆⁺ signal.³ The unfocused pump and focused (by a lens with a focal length of 50 cm) probe beams were collinearly combined and sent into the photoionization chamber. The probe beam polarization was set by a half-wave plate to an angle of 54.7° (magic angle) relative to the pump beam polarization; this eliminates time dependences that could originate from molecular rotation. Time zero was determined as the maximum of the transient ion signal for Xe (introduced through a second needle valve, pressure 10^{−5} mbar), which is due to pure nonresonant (2+2) multiphoton ionization under the given conditions. Two ion signals (normally a Cr(CO)₆⁺ peak—which has a very short-lived neutral precursor³—and one of the Ni-containing signals) were recorded simultaneously by means of two boxcar integrators. This method provided synchronization of different scans with an accuracy of ±2 fs. For each delay the data were integrated over 1 s (1000 pulses), and the scans containing 100–200 such points were repeated; typically 10 scans were averaged before evaluating them for the time constants.

The probe laser alone produced a small ion yield (few percent of the signal maxima) that was subtracted from the signals. With the pump laser alone no ions were detected.

The five ion signals Ni(CO)_k⁺, *k* = 4–0, differ in their time behavior. They can be simulated by assuming that each ion (mass *m*) is generated with probability (cross-section) ^{*m*}σ_{*i*} from one or several locations (observation windows) *i* on the potential energy surface(s) and that the windows *i* are sequentially reached and passed in a time (“lifetime”) τ_{*i*}. The population in each window is modeled by rate equations; their solutions are a sum

TABLE 1: Bond Dissociation Energies (in eV) of Ni(CO)₄ and Ni(CO)_k⁺^a

	<i>k</i>	4	3	2	1
Ni(CO) _{<i>k</i>−1} −CO		1.1 ± 0.1	0.8 ± 0.3	2.3 ± 0.7	1.3 ± 0.7
[Ni(CO) _{<i>k</i>−1} −CO] ⁺		0.54	1.32	1.96	2.28

^a Ionization energy 8.90 eV (from the photoelectron spectrum²⁷); mean energy carried away by the first CO eliminated 0.5 eV¹⁷; laser photon 4.65 eV (267 nm), 4.77 eV (260 nm), 4.49 eV (275 nm), emitting Ni(CO)₃ state about 2.2 eV (from the short-wavelength edge near 560 nm).¹²

of time-dependent exponentials.²³ The signals are hence represented by a sum of exponentials (with time constants τ_{*i*}) convoluted by the (Gaussian) pump and probe pulses (for details see).²³ The ^{*m*}σ_{*i*} are results of a fit procedure. The sub-ps times τ₄ and τ₅ are long enough to be directly evaluated from the doubly exponential tails of Ni(CO)₃⁺ and Ni(CO)₂⁺ at times longer than the pulse length (corresponding to a multiple of τ_{*i*}). Much shorter lifetimes only give rise to a delayed (by τ_{*i*}) signal without affecting its Gaussian shape. τ₁ was deduced in this way from the parent ion signal. Beyond evaluation of the delays and exponential tails, the simulation of the full signals is a check for consistency. It thus turned out that two additional time constants (τ₂, τ₃) were necessary to simultaneously account for the shift and compactness of the Ni(CO)⁺ and Ni⁺ signals. The rate-equation model using the first five time constants (Table 3 below) connecting six observation windows (locations L₁ to L₆) with relative ionization cross-sections ^{*m*}σ_{*i*} (Table 3) then quite well reproduces the signals in the time range until several picoseconds. In this simulation the L₆ lifetime was assumed to be infinite. Indeed, τ₆ is much longer than the preceding times. It was separately determined from the decay of the signals Ni(CO)_{*k*}⁺, *k* = 3–1 in the range of 10–500 ps.

Variation of the pump intensity by a factor of 3 did not change the shapes of the signals. This confirms that the molecules are pumped by single-photon excitation. A similar variation of the probe had an influence on the shapes, as expected since ionization from, for example, the product ground state (giving rise to a pedestal) with its lower electronic energy requires a larger number of probe photons than ionization from the initially excited state; however, the resulting time constants were not affected.

Whereas for evaluating ^{*m*}σ_{*i*} and τ_{*i*} it is not necessary to know anything about the mechanism of ionization and fragmentation, such knowledge is helpful for localizing the observation windows. Briefly (for details, see refs 3, 5, and 23), every neutral precursor can in general give rise to several ions; fragmentation takes place in the ion typically within nanoseconds and is caused by excess energy of the ion. Among the three origins of this energy, only one is important for assignments in the nickel carbonyl system [a second one, namely absorption of probe laser radiation by an ion, is necessary to explain the observation of Ni⁺, which requires more energy than that of the pump photon and the ionization energy (altogether corresponding to 6 probe photons)]: In the vertical ionization process, vibrational excess energy released in the neutral during electronic relaxation is largely (the part contained in Franck–Condon inactive modes) or completely (in the case of a compact wave packet) transferred to the ion. Ionic fragmentation can thus give a hint on vibrational energy of the neutral, hence also on electronic energy (since the sum is constant) and on the location on the surface. Therefore it is helpful to consider the energetics. The bond dissociation energies are given in Table 1. For the neutral molecule we took those of Lineberger and colleagues²⁵ modified by Hepburn and

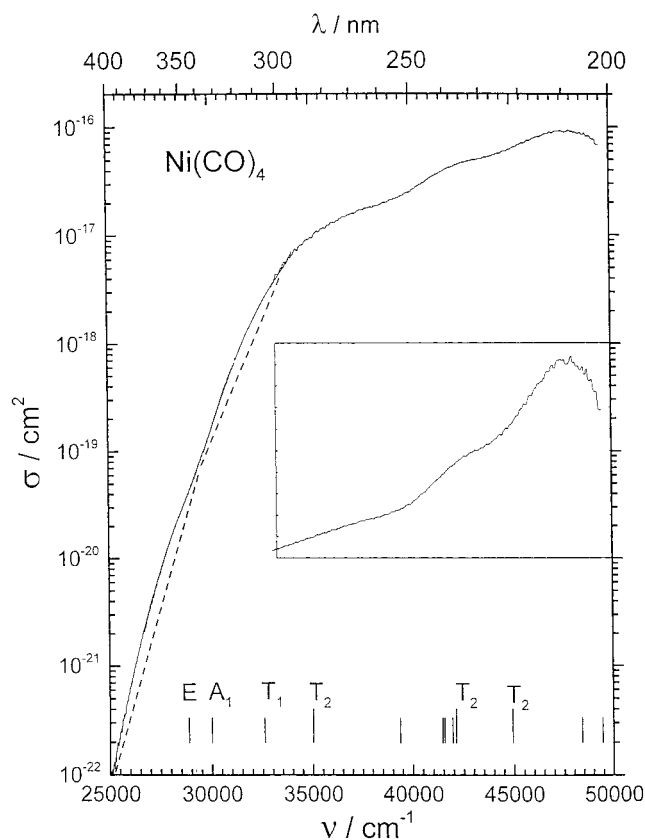


Figure 1. Ultraviolet spectrum of Ni(CO)₄ in the gas phase. The overlapping traces are from different sources: The parts below 10^{-17} cm^{-2} were recorded with saturated vapor pressure (500 mbar, filled up to 1 bar with CO) at 297 K in cells of 1, 10, and 100 mm length; the spectral slit width was 0.5 nm (40 cm^{-1}). The part with intensity above 10^{-17} cm^{-2} was taken with kind permission from ref 18. This part (which was slightly smoothed) is also shown in the *inset* in a linear scale (from 0 to 10^{-16} cm^{-2} , abscissa as in the main part). The broken straight lines were only drawn to help recognize the shoulders. The vertical bars indicate the band locations calculated by CAS-PT2.⁹

colleagues.¹⁷ Those of the ions are from the differences of the corresponding appearance potentials (estimated error 0.15 eV).²⁶

Ni(CO)₄ (Alfa Products) was used after degassing without further purification.

Results

The lowest excited states play an important role in electronic relaxation. They are only connected by symmetry-forbidden transitions to the ground state. Therefore we measured in the gas-phase UV spectrum also the weak precursor bands not reported before (Figure 1). Obviously the states $1E$ and $1T_1$ predicted by the CAS-PT2 calculation (energies including correlation of $3d$ and $3s$, $3p$ electrons in ref 9) can be assigned to the two long-wavelength shoulders, whereas the $2A_1$ state is not resolved. The calculation without this correlation²⁰ and the predictions by time-dependent DFT²¹ and the SAC-CI approach¹⁵ do not so well agree with this long-wavelength part.

Figure 2 shows the time-dependent ion signals. Because the signals in this figure are normalized, we give in Table 2 the actual fragmentation patterns at two different delay times. It shows that Ni(CO)₂⁺ is the strongest signal at all times, although the degree of fragmentation increases with time.

Whereas the parent ion only shows a slight delay versus the instrumental function (broken line in Figure 2) and decays to zero, all the other signals more slowly decay to nonvanishing long-time values (“pedestals”). The logarithmic plots, in which

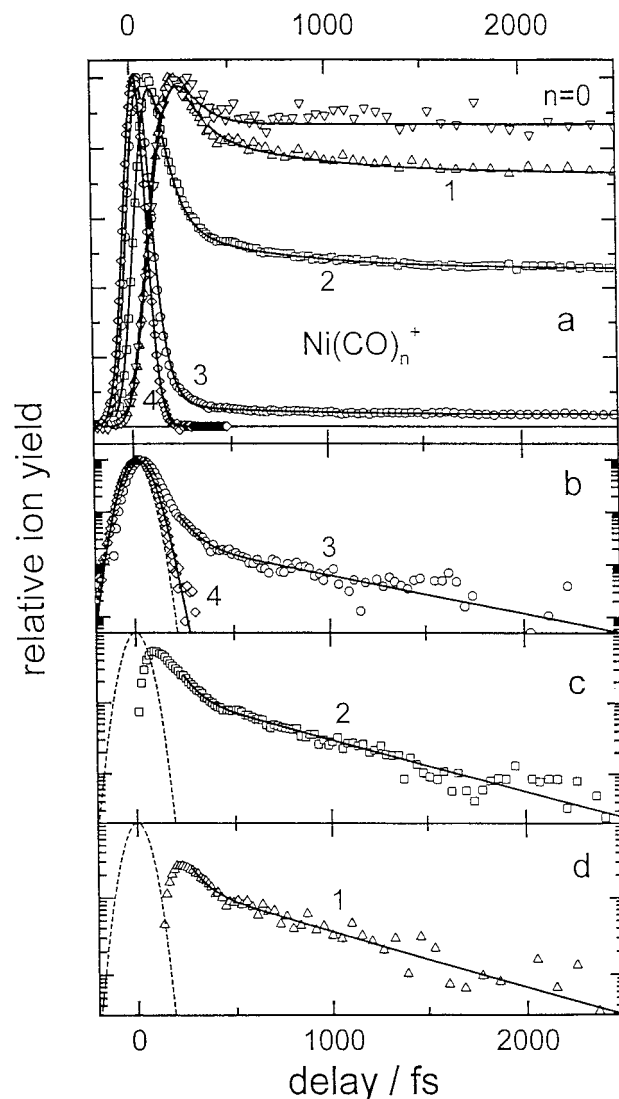


Figure 2. Time-resolved normalized signals Ni(CO)_n⁺ in linear (top) and logarithmic (bottom) scale; in the latter part, the long-time values of the signals have been subtracted. The solid lines result from simulation with the constants of Table 3 (top) and from doubly exponential fitting with τ_4 and τ_5 (bottom). The dotted line indicates the instrumental function (pump–probe correlation function).

TABLE 2: Relative Signal Intensities at Two Different Delay Times

	Ni(CO) ₄ ⁺	Ni(CO) ₃ ⁺	Ni(CO) ₂ ⁺	Ni(CO) ⁺	Ni ⁺
20 fs	0.024	0.565	1	0.04	0.056
700 fs	0	0.026	1	0.35	0.04

the pedestals have been subtracted, show that this decay is (at least) doubly exponential with the same two time constants (70 and 600 fs) for all fragment signals. Beyond this time scale, these fragment signals furthermore show a decay in the picosecond range, although with small amplitude (Figure 3). This slowest part depends on the pump wavelength (Figure 3). Thereafter, the signals stay constant over more than 500 ps. As described in the foregoing section, the signals can be simulated by assuming consecutive population of locations i with lifetimes τ_i on the potential energy surfaces of the neutral molecules. Table 3 shows these times. It also gives the relative cross-sections (probabilities) ${}^m\sigma_i$ to generate from location i an ion m . These values also indicate which time constant is contained in which of the signals. For a given i (that is, a column of the

TABLE 3: Time Constants τ_i to Pass and Leave Location i and Relative Ionization Cross-Sections ${}^m\sigma_i$ to Generate Ion m (Given by the Formula) from Location i^a

i	1	2	3	4	5	6
τ_i/fs	22 ± 2	50 ± 10	60 ± 10	70 ± 10	600 ± 100 (-; 730)	$55 \times 10^3 \pm 10\%$ (42×10^3 ; 113×10^3)
$\text{Ni}(\text{CO})_4^+$	1	0	0	0	0	0
$\text{Ni}(\text{CO})_3^+$	1.0	0.732	0.00242	0.022	0.0212	0.0128
$\text{Ni}(\text{CO})_2^+$	0	1.0	0.993	0.518	0.403	0.328
$\text{Ni}(\text{CO})^+$	0	0.0	0.10	1	0.43	0.365
Ni^+	0	0	0	1	0.434	0.434

^a Time constants in τ_5 and τ_6 parentheses were measured with pump wavelength 260 (τ_5 not evaluated) and 276 nm instead of 267 nm.

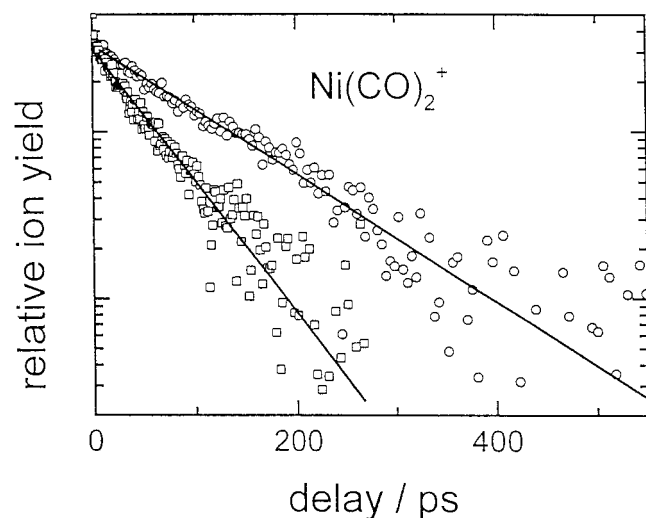


Figure 3. Decay in picosecond range, shown with example of $\text{Ni}(\text{CO})_2^+$ signal for two different pump wavelengths (\square , 267 nm; \circ , 276 nm). The long-time values (pedestals) of the signals have been subtracted.

table), the ${}^m\sigma_i$ roughly indicate the fragmentation pattern for the location i . In the next section we will try to assign these locations.

Discussion

Assignment. The fact that the $\text{Ni}(\text{CO})_3^+$ signal has a nondecaying “pedestal” means that at least part of the neutral $\text{Ni}(\text{CO})_3$ is stable over more than 1 ns. This means that it is in an excited state, since in the ground state it would very rapidly dissociate already within picoseconds or faster, given the excess energy with which it would be formed (about 3 eV; see the energetics in Table 1), which is much larger than its dissociation energy (about 0.8 eV; Table 1). From the energetics of the ions we can even conclude more: The ions $\text{Ni}(\text{CO})_3^+$ and $\text{Ni}(\text{CO})_2^+$ would not be detected if formed from the ground state of $\text{Ni}(\text{CO})_3$ since with the excess energy (around 3 eV, taken over to the ion in the ionization process; see Experimental Method) these ions would never survive the nanosecond times of extraction from the ion source; actually $\text{Ni}(\text{CO})_2^+$ is even the strongest signal at any positive delay time. Because τ_2 – τ_6 can be extracted from these signals, these time constants (and the preceding one, of course) cannot reflect the kinetics of ground-state $\text{Ni}(\text{CO})_3$ but that of its excited state and its precursor(s).

In the next paragraph we will assign τ_6 to the decay of excited $\text{Ni}(\text{CO})_3$. Hence τ_5 (= 600 fs) will reflect its formation. Because this and all the preceding times are clearly below 1 ps and because intersystem crossing is unlikely to be 3 orders of magnitude faster than in $\text{Fe}(\text{CO})_4$ where it takes more than 500 ps,⁵ the excited $\text{Ni}(\text{CO})_3$ state must belong to the singlet manifold and is most likely S_1 . In principle, τ_5 could reflect a

$S_n \rightarrow S_1$ relaxation. However, the fragmentation pattern changes noticeably during this process (compare the columns ${}^m\sigma_5$ and ${}^m\sigma_6$ in Table 3), which would be unexpected for two states of similar electronic energy. Therefore we assign τ_5 to the time of dissociation from the last populated excited state of $\text{Ni}(\text{CO})_4$. This is also supported by the weak wavelength dependence as discussed in the next paragraph. The preceding time constants τ_1 – τ_4 then must represent processes in the intact $\text{Ni}(\text{CO})_4$. τ_1 is certainly the time for leaving the Franck–Condon region or the initially excited $1T_2$ state. τ_2 – τ_4 are then probably times for traveling along the next lower surfaces ($1T_1$, $2A_1$, and $1E$) and (consistent with the statement above) τ_5 the time of departure from the lowest excited state ($1E$), the only state that correlates with S_1 of the product $\text{Ni}(\text{CO})_3$.¹⁵ Further details will be considered in the section on potential energy surfaces and Figure 4.

The sixth relaxation takes place in a much longer time scale ($\tau_6 = 55$ ps). As mentioned, it must be a process involving excited $\text{Ni}(\text{CO})_3$. It can either be a slow electronic relaxation between two excited states ($S_n \rightarrow S_1$) or intersystem crossing ($S_1 \rightarrow T_1$), or a more or less thermal process stimulated by excess vibrational energy. In fact, intersystem crossing was calculated in similar compounds to take several tens of picoseconds (see, e.g., ref 28) and measured in $\text{Fe}(\text{CO})_4$ to take 8 ps in solution;²⁹ on the other hand, in the latter case the process was accelerated by solvent-induced (time-dependent) surface crossing.²⁹ To decide between electronic relaxation and a thermal process, we altered the excess energy by about ± 0.15 eV by taking different pump wavelengths (260 and 276 nm). τ_6 changed thereby to 42 and 113 ps, respectively. That is, the process is activated or even endothermic. Hence we can exclude intersystem crossing, which is not expected to need activation energy. Also, $S_n \rightarrow S_1$ relaxation should be a nonactivated process, because an easily accessible intersection between S_2 (which might also be populated in the dissociation process)¹³ or S_n and the JT split S_1 ¹⁵ can be expected. (In a similar way, the weak wavelength dependence of τ_5 makes it unlikely that this preceding process represents $S_n \rightarrow S_1$ relaxation, but more probably dissociation as suggested.) The reverse process, $S_1 \rightarrow S_2$, cannot be excluded, although it would be unusual. We prefer to assign τ_6 to endothermic dissociation of hot $\text{Ni}(\text{CO})_3$ (S_1) molecules to excited $\text{Ni}(\text{CO})_2$. To explain why this decay leads to a nonvanishing value of the $\text{Ni}(\text{CO})_3^+$ signal (Figure 2), we postulate that only part of the excited tricarbonyl molecules have excess energy sufficient for the endothermic dissociation to $\text{Ni}(\text{CO})_2$ (S_1). [Note that dissociation to ground-state $\text{Ni}(\text{CO})_2$, which is exothermic (Table 1), would not offer the possibility of consuming only a fraction of the tricarbonyl and thus could not explain our signals.] It is interesting that a component of the luminescence seen on 248-nm irradiation of $\text{Ni}(\text{CO})_4$ is believed to be due to $\text{Ni}(\text{CO})_2$;¹³ to judge from the emission maxima, the excitation energy of the dicarbonyl is smaller by 0.14 eV than that of the tricarbonyl, so that dissociation from

S_1 to S_1 would still be endothermic by about 0.95 eV. Correlation rules also suggest that there is no direct connection of S_1 of one molecule with S_0 of the other.³⁰

Luminescence Revisited. In view of these results it seems worth reconsidering the published results on luminescence observed on laser irradiation of Ni(CO)₄. The lowest excited singlet state ($1E$) of Ni(CO)₄ correlates with S_1 of Ni(CO)₃, which belongs to the degenerate species $1E''$ in D_{3h} . This can be recognized from the published SAC-CI¹⁵ or X α ³⁰ calculations, but according to Daniel et al.¹⁶ also from simple correlation rules: because the S_0 of Ni(CO)₃ is nondegenerate, it can only correlate with one state (S_0 , of course) of Ni(CO)₄. Hence S_1 of Ni(CO)₄ must correlate with excited Ni(CO)₃. However, the same kind of argument applies to all $M(CO)_{n-1}$ resulting from closed-shell $M(CO)_n$; it was used to explain why $M(CO)_{n-1}$ was initially formed in its S_1 state in the carbonyls of Cr, Mo, W,⁴ Fe,⁵ Mn, and Re.⁶ This S_1 state relaxed to S_0 within 40–70 fs, a time range that explains why no luminescence was found from these unsaturated carbonyls. This ultrafast process is brought about by an easily accessible real crossing (conical intersection) of the S_1 and S_0 surfaces: In a highly symmetric geometry [T_d for Fe(CO)₄, D_{3h} at least locally in the other cases] the lowest singlet state is degenerate; the JT theorem predicts that it is split by a suitable distortion (a pseudorotation coordinate), the components just being S_1 and S_0 in the less symmetric geometry.

These cases demonstrate that correlation is not sufficient to predict luminescence. Therefore we check for the presence of any JT-induced surface intersection in planar symmetric (D_{3h}) Ni(CO)₃. The first excited state is degenerate and antisymmetric to the plane ($1E''$). It is split by a planar distortion (e') involving both bond lengths and angles.¹⁵ The resulting states ($1B_1$ and $1A_2$ in C_{2v}) are again antisymmetric to the plane and hence do not include the ground state ($1A_1$). So JT splitting does not connect S_1 with S_0 in Ni(CO)₃. This is probably a general rule for all 16-electron complexes with coordination number 3 or less (in contrast to higher coordination, see above). It is a necessary condition for observation of luminescence in such systems.

In the context of the S_1 degeneracy it is worth noting that below S_1 a triplet state must exist with the same symmetry species $^3E''$ and probably a similar JT splitting. Intersystem crossing perhaps takes place within a few nanoseconds, that is, in a time much shorter than the luminescence lifetime $\tau_{lum} > 10 \mu s$ observed in ref 12 and also shorter than the radiative lifetime of S_1 . The value of τ_{lum} is also more consistent with phosphorescence than with a singlet–singlet transition. In this context an apparent inconsistency in the literature is interesting: Preston and Zink reported a luminescence lifetime τ_{lum}' of about 200 ns¹⁴ or, extrapolated to pressure $p = 0$ from their p -dependent data, 300 ns;³¹ the slope in this dependence corresponds to a deactivation with around 10^{-2} the gas kinetic rate. This is too fast to represent quenching of a triplet. Extrapolating singlet-quenching data to $p = 0$ will result in the singlet lifetime, which should therefore be assigned to the value $\tau_{lum}' = 300$ ns. In these experiments, the triplet was apparently not populated, because at the high pressures used (several hundred mbar) S_1 was quenched before intersystem crossing. In contrast, in the experiments of Schröder and colleagues¹⁸ with their pressure in the microbar range, S_1 quenching could not compete with intersystem crossing, and $\tau_{lum} > 10 \mu s$ can therefore be considered as the phosphorescence time.

JT splitting of the S_1 state gives rise to an energy minimum in the $1B_1$ sheet of the split surface that is displaced along an

e' coordinate.¹⁵ (More precisely, because the coordinate is degenerate, it is a ring channel around the conical intersection.) If splitting and displacement were large enough, another type of easily accessible intersection with the ground state could arise; if the effect is smaller, the crossing will be in the rising outer wing of the $1B_1$ surface and may be energetically inaccessible. Obviously the latter case applies to Ni(CO)₃, because no luminescence would be observed otherwise. The situation can, however, be different at a time before dissociation is complete; JT splitting along the e coordinate (in C_{3v} , corresponding to e' in D_{3h}) should also exist in such earlier phases. If such a conical intersection would energetically be accessible already in the intact molecule, it would lower the quantum yield of dissociation (which is believed, however, to be near 1 for all metal carbonyls if recombination is avoided).² If it is accessible (via a distortion of species e in C_{3v}) after some stretching of a Ni–CO bond, it will lead to a branching between excited and ground-state Ni(CO)₃. In fact, the photofragment results of Hepburn and co-workers were best reproduced with the assumption of a branching (with the S_1 state dominating).¹⁷ Such a crossing may also be responsible for the efficient recombination in a matrix³² and the fast quenching of luminescence by collisions with CO;³³ this quenching is thus again interpreted as taking place before intersystem crossing.

It is worth noting that such branching of the 600-fs dissociation step does not contradict the statement (Assignment section) that the *observed* kinetics was not from S_0 of Ni(CO)₃: If any processes in this state, such as thermal dissociation, are much faster than the preceding 600-fs process (which is conceivable because of the high excess energy), they cannot be resolved owing to a general principle of kinetics; the signals from S_0 would then only show the 600-fs time constant.

The observation of the long-lived Ni(CO)₃⁺ signal [and of Ni(CO)₃ luminescence in refs 12–14] has also another implication: it clearly demonstrates that only a single CO is photochemically eliminated. For the group-6 carbonyls $M(CO)_6$ we drew the same conclusion from the observation of coherent oscillations in $M(CO)_5$,^{3,4} which would be difficult to assign to any other species, and for Fe(CO)₅ from the suppression of any second step in solution;⁵ only thermal processes are suppressed by cooling in the condensed phase. All this is in agreement with the common opinion on metal carbonyl photochemistry.² But it is in contrast to a claim that even naked Fe atoms were produced in a subpicosecond time scale by two-photon excitation of Fe(CO)₅ at 400 nm.¹¹

Potential Energy Surfaces. We can now come back to the early phases of the photoreaction dynamics. Although the following assignment of $\tau_2 - \tau_4$ must be considered tentative, we can draw some conclusions on the potential energy surfaces. Arguing can be brief since it is similar, as in our work on $M(CO)_6$,⁴ $\tau_1 - \tau_4$ are very short, shorter than a vibrational period that would, for example, be around 80 fs for Ni–C stretching. For τ_1 this is possible if the wave packet is accelerated from the outset; this limits the choice of coordinates to totally symmetric and JT active ones. (In a highly symmetric molecule the initial slope is zero along the other coordinates.) Any change of electronic state can take place in a time as short as $\tau_2 - \tau_4$ only if the wave packet passes through an easily accessible conical intersection. Such features as well as an initial nonzero slope are provided by JT splitting of the degenerate excited states. This is schematically indicated in the inset of Figure 4. JT active coordinates have species e for E states and species e and t_2 for triply degenerate states. Whereas e -type distortion corresponds to bending, t_2 also comprises stretching; dissociation

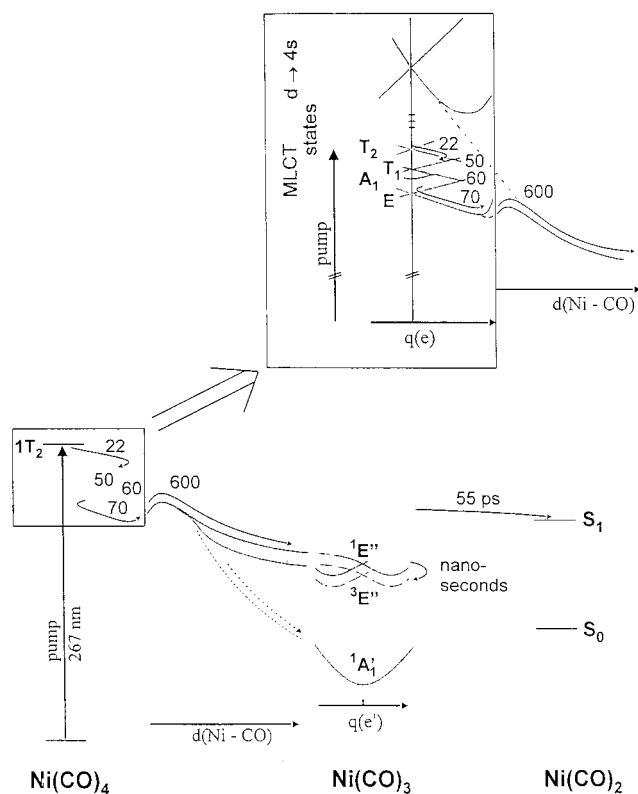


Figure 4. Suggested potential energy surfaces and pathways (time constants in femtoseconds, except the last one) in the nickel carbonyl system. The branching of the solid lines along the dissociation coordinate is meant to indicate the Jahn–Teller (JT) splitting along an e coordinate, whereas the broken line indicates the suggested (less probable) pathway via a conical intersection to the ground state. The 55-ps process is suggested to involve only the $\text{Ni}(\text{CO})_3$ molecules in S_1 with high vibrational excess energy. The inset gives details in the intact $\text{Ni}(\text{CO})_4$. The suggested initial relaxation coordinate is an e -type bending, which is JT active. The broken line coming down from the $d \rightarrow 4s$ states shows the origin of the avoided crossing giving rise to a small barrier.

of a single Ni–CO corresponds to a superposition of a t_2 and an a_1 coordinate. It is very interesting that the lowest excited state ($1E$) is only distorted by bending (resulting symmetry D_{2d}); because bending cannot infinitely continue, we can expect a minimum in this direction. If the molecule followed a t_2 coordinate from the outset (such as in the calculation of ref 15, which suggested dissociation from the $1T_1$ state), it would be difficult to understand why it would not just go on along this coordinate to dissociation but instead meets a barrier (see below). We also suggest that in the higher states the slope is steeper in the direction of the e -type bending than of t_2 (and other) stretching, so that the molecule prefers relaxation along the former coordinate. This assumption can explain why the molecule finds the minimum, although according to the calculation¹⁵ a direct dissociation (from T_1) would be possible.

We suggest that τ_4 , the last relaxation time before dissociation, represents to a large part the time of traveling along the $1E$ surface. The preceding two times could then involve the $1T_1$ and $2A_1$ surfaces. However, they may also reflect a change of direction of the relaxation coordinate. (In previous work, we found that the detection method can be sensitive for such changes.)^{23,34}

In an attempt to find any anisotropy and its decay we varied the relative polarization of pump and probe beams. But the time dependence of the signals was independent of polarization from the outset. This is a support for motion along JT active

coordinates: they are spatially degenerate, so that there is no preference of any direction of acceleration, although the linear polarization of the pump laser must initially generate an electronic anisotropy. The similar results for the group-6 metal carbonyls were interpreted in the same way.⁴

Density-functional calculations on group-6 carbonyls placed the strongly repulsive LF states above most of the (basically not dissociative) MLCT states and suggested that the molecules dissociate by passing from an MLCT surface via an avoided crossing to a steeply descending LF surface.^{7,8} The avoided crossing can in principle give rise to a barrier, in particular if the LF states are very high in energy. To judge from the short times for the dissociation step of most carbonyls investigated (< 100 fs),⁶ the activation energy is negligible for them. In contrast, the much slower dissociation step in $\text{Ni}(\text{CO})_4$ ($\tau_5 = 600$ fs) suggests a barrier. It is indicated in Figure 4. The role of the LF states [which do not exist in $\text{Ni}(\text{CO})_4$ because of the full d shell] can be taken by $d \rightarrow 4s$ states that lie at the upper end of the MLCT states.¹⁵ A confirmation is the slight lengthening of τ_5 (to about 700 fs) observed when we decreased the excess energy by 0.16 eV by increasing the pump wavelength to 276 nm. To conclude, we suggest that the molecule is initially guided by a steep slope along an e -type bending coordinate until it reaches a minimum; only then, to find out from there, it changes direction versus dissociation and climbs over a small barrier.

In view of the long dissociation time, a vibrational structure could be expected in the longest-wavelength UV band of $\text{Ni}(\text{CO})_4$. None was found, however (Figure 1). It may be worth recording a spectrum at low temperature.

At first sight it also seems plausible to connect with the long dissociation time the observation that the energy in the photo-fragment CO was more or less statistically distributed (Boltzmann distributions with not very different temperatures for translation, rotation, and vibration).¹⁷ However, 600 fs is much too short to equilibrate, for instance, the CO stretch with the lower-frequency vibrations; even with collisions in solution no equilibrium between high- and low-frequency vibrations is reached over many tens of picoseconds (in the electronic ground state of metal carbonyls) since two time scales can be distinguished for relaxation from vibration to translation (see, e.g., refs 35 and 36). We prefer to attribute the high rotational temperatures to the involvement of bending caused by JT distortion (leading to a noncollinear MCO arrangement) before a practically impulsive dissociation, and the CO vibration to the initial excitation of an MLCT state (which is CO antibonding). In this model it is also easy to understand why CO rotation was relatively cold in dissociation of $\text{W}(\text{CO})_6$ ³⁷ (nearly linear WCO group during dissociation),⁴ whereas the statistical model probably has difficulties explaining this difference.

Conclusion

The most striking difference in the photochemistry of $\text{Ni}(\text{CO})_4$ and that of other carbonyls is the luminescence observed in the nickel system. Correlation rules predict that photolysis of all $\text{M}(\text{CO})_n$ initially forms $\text{M}(\text{CO})_{n-1}$ in its first excited singlet state. However, for $n = 5$ or 6 the JT effect in the 16-electron complex connects S_1 with S_0 via a conical intersection, whereas according to group theory such a connection is not predicted for $n = 4$ [$\text{Ni}(\text{CO})_3$] and lower coordination, although JT distortion exists too. The difference of lifetimes is more than 8 orders of magnitude. [We suggest, however, intersystem crossing $S_1 \rightarrow T_1$ of $\text{Ni}(\text{CO})_3$ to take place in a nanosecond time scale, before luminescence.] The long lifetime of excited $\text{Ni}(\text{CO})_3$ should also

leave signatures in the rate and pathway of bimolecular reactions. But apparently this question has not found attention so far.

It is also surprising that the dissociation step in Ni(CO)₄ takes an order of magnitude longer (600 fs) than in other mononuclear carbonyls, although the first bond dissociation energy (in the ground state) is smallest in the nickel carbonyl. We explain it by a postulated small barrier arising from an avoided crossing of an MLCT surface with a σ -antibonding $d \rightarrow 4s$ surface; in Ni(CO)₄ these antibonding states are probably higher in energy (causing also a higher barrier) than the (antibonding) LF states in most other carbonyls. A significant contribution to make this barrier noticeable may come from a minimum before, which may arise from a slope that is steeper along a JT active bending direction than along the dissociation coordinate.

Despite these differences among the metal carbonyls, their photoreaction dynamics seem to follow one common mechanism. It involves (1) initial relaxation to other MLCT states along a continuous path through JT-induced conical intersections to one of the lowest such states; JT active coordinates strongly influence the direction of motion, (2) thereafter passing over to a steeply repulsive surface, typically via an avoided crossing, eliminating a single CO; (3) the dissociation resulting in M(CO)_{n-1} in its S₁ state, which is subject to the JT effect; this effect sometimes creates an ultrafast channel down to S₀; (4) thermal elimination of additional ligands depending on excess energy; (5) all processes below about 1 ns taking place in the singlet manifold.

Acknowledgment. We thank H. Schröder and J. I. Zink for helpful discussions and information.

References and Notes

- (1) Wrighton, M. S. *Chem. Rev.* **1974**, *74*, 401.
- (2) Geoffroy, G. L.; Wrighton, M. S. *Organometallic Photochemistry*; Academic Press: New York, 1979.
- (3) Trushin, S. A.; Fuss, W.; Schmid, W. E.; Kompa, K. L. *J. Phys. Chem. A* **1998**, *102*, 4129.
- (4) Trushin, S. A.; Fuss, W.; Kompa, K. L.; Schmid, W. E. *Chem. Phys.* **2000**, *259*, 313.
- (5) Trushin, S. A.; Fuss, W.; Schmid, W. E.; Kompa, K. L. *J. Phys. Chem. A* **2000**, *104*, 1997.
- (6) Fuss, W.; Trushin, S. A.; Schmid, W. E. *Res. Chem. Intermed.* **2000**, *14*, in press.
- (7) Pollak, C.; Rosa, A.; Baerends, E. J. *J. Am. Chem. Soc.* **1997**, *119*, 7324.
- (8) Baerends, E. J.; Rosa, A. *Coord. Chem. Rev.* **1998**, *177*, 97.
- (9) Pierloot, K.; Tsokos, E.; Vanquickenborne, L. G. *J. Phys. Chem.* **1996**, *100*, 16545.
- (10) Rubner, O.; Engel, V.; Hachey, M. R.; Daniel, C. *Chem. Phys. Lett.* **1999**, *302*, 489.
- (11) Bañares, L.; Baumert, T.; Bergt, M.; Kiefer, B.; Gerber, G. *J. Chem. Phys.* **1998**, *108*, 5799.
- (12) Rösch, N.; Kotzian, M.; Jörg, H.; Schröder, H.; Rager, B.; Metev, S. *J. Am. Chem. Soc.* **1986**, *108*, 4238.
- (13) Reiner, H.; Wittenzellner, C.; Schröder, H.; Kompa, K. L. *Chem. Phys. Lett.* **1992**, *195*, 169.
- (14) Preston, D. M.; Zink, J. I. *J. Chem. Phys.* **1987**, *91*, 5003.
- (15) Hada, M.; Hidaka, M.; Nakatsuji, H. *J. Chem. Phys.* **1995**, *103*, 6993.
- (16) Daniel, C.; Benard, M.; Dedieu, A.; Wiest, R.; Veillard, A. *J. Phys. Chem.* **1984**, *88*, 4805.
- (17) Schlenker, F. J.; Bouchard, F.; Waller, I. M.; Hepburn, J. W. *J. Chem. Phys.* **1990**, *93*, 7110.
- (18) Kotzian, M.; Rösch, N.; Schröder, H.; Zerner, M. C. *J. Am. Chem. Soc.* **1989**, *111*, 7687.
- (19) Schreiner, A. F.; Broen, T. L. *J. Am. Chem. Soc.* **1968**, *90*, 3366.
- (20) Roos, B. O.; Andersson, K.; Fülcher, M. P.; Serrano-Andrés, L.; Pierloot, K.; Merchán, M.; Molina, V. *J. Mol. Struct. (THEOCHEM)* **1996**, *388*, 257.
- (21) Van Gisbergen, S. J. A.; Groeneveld, J. A.; Rosa, A.; Snijders, J. G.; Baerends, E. J. *J. Phys. Chem. A* **1999**, *103*, 6835.
- (22) Fuss, W.; Schmid, W. E.; Trushin, S. A. *ISRAPs Bull.* **2000**, *11*, 7.
- (23) Fuss, W.; Schmid, W. E.; Trushin, S. A. *J. Chem. Phys.* **2000**, *112*, 8347.
- (24) Trushin, S. A.; Fuss, W.; Schmid, W. E. *Phys. Chem. Chem. Phys.* **2000**, *2*, 1435.
- (25) Stevens, A. E.; Feigerle, C. S.; Lineberger, W. C. *J. Am. Chem. Soc.* **1982**, *104*, 5026.
- (26) Schildcrout, S. M.; Pressley, G. A., Jr.; Stafford, F. E. *J. Am. Chem. Soc.* **1967**, *89*, 1617.
- (27) Decleva, P.; Fronzoni, G.; De Alti, G.; Lisini, A. *J. Mol. Struct. (THEOCHEM)* **1991**, *226*, 265.
- (28) Heitz, M.-C.; Daniel, C. *J. Am. Chem. Soc.* **1997**, *119*, 8269.
- (29) Harris, C. B. Talk on Fourth Symposium on Selective Reactions in Metal-Activated Molecules, 2000, Würzburg, Germany.
- (30) Rösch, N.; Jörg, H.; Kotzian, M. *J. Chem. Phys.* **1987**, *86*, 4038.
- (31) Zink, J. I. Personal communication.
- (32) Turner, J. J.; Burdett, J. K.; Perutz, R. N.; Poliakov, M. *Pure Appl. Chem.* **1977**, *49*, 271.
- (33) Schröder, H. Personal communication.
- (34) Trushin, S. A.; Diemer, S.; Fuss, W.; Kompa, K. L.; Schmid, W. E. *Phys. Chem. Chem. Phys.* **1999**, *1*, 1431.
- (35) Lian, T.; Bromberg, S. E.; Asplund, M. C.; Yang, H.; Harris, C. B. *J. Phys. Chem.* **1996**, *100*, 11994.
- (36) Ko, S.-B.; Yu, S.-C.; Hopkins, J. B. *Bull. Korean Chem. Soc.* **1994**, *15*, 762.
- (37) Holland, J. P.; Rosenfeld, R. N. *J. Chem. Phys.* **1988**, *89*, 7217.